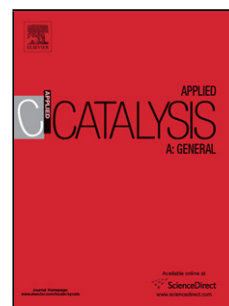


# Journal Pre-proof

Improving the synthesis of Zn-Ta-TUD-1 for the Lebedev process using the Design of Experiments methodology

Guillaume Pomalaza (Investigation) (Methodology) (Formal analysis) (Writing - original draft), Mickaël Capron (Supervision) (Funding acquisition), Franck Dumeignil (Supervision) (Writing - review and editing) (Funding acquisition) (Validation)



PII: S0926-860X(19)30541-1

DOI: <https://doi.org/10.1016/j.apcata.2019.117386>

Reference: APCATA 117386

To appear in: *Applied Catalysis A, General*

Received Date: 12 October 2019

Revised Date: 22 December 2019

Accepted Date: 24 December 2019

Please cite this article as: Pomalaza G, Capron M, Dumeignil F, Improving the synthesis of Zn-Ta-TUD-1 for the Lebedev process using the Design of Experiments methodology, *Applied Catalysis A, General* (2019), doi: <https://doi.org/10.1016/j.apcata.2019.117386>

This is a PDF file of an article that has undergone enhancements after acceptance, such as the addition of a cover page and metadata, and formatting for readability, but it is not yet the definitive version of record. This version will undergo additional copyediting, typesetting and review before it is published in its final form, but we are providing this version to give early visibility of the article. Please note that, during the production process, errors may be discovered which could affect the content, and all legal disclaimers that apply to the journal pertain.

© 2019 Published by Elsevier.

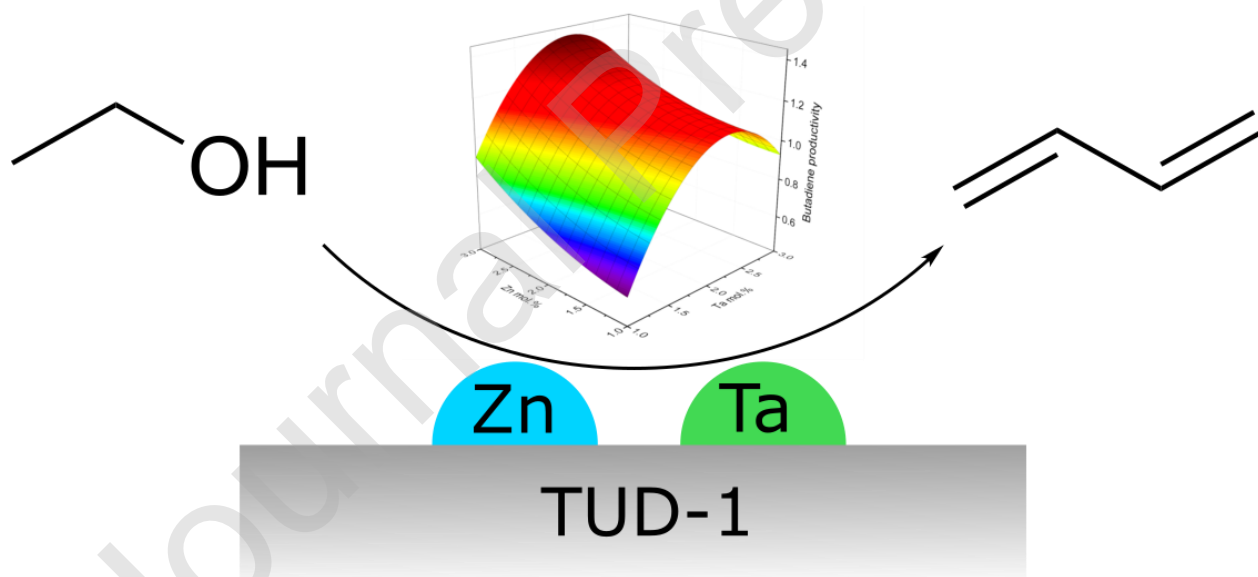
# Improving the synthesis of Zn-Ta-TUD-1 for the Lebedev process using the Design of Experiments methodology

Guillaume Pomalaza,<sup>a</sup> Mickaël Capron,<sup>a</sup> Franck Dumeignil<sup>a,\*</sup>

<sup>a</sup>Univ. Lille, CNRS, Centrale Lille, ENSCL, Univ. Artois, UMR 8181 – UCCS – Unité de Catalyse et Chimie du Solide, F-59000 Lille, France

\*corresponding author, franck.dumeignil@univ-lille.fr

## Graphical abstract



## Highlights

- Zinc-tantalum on mesoporous silica TUD-1 catalyst showed remarkable activity in the conversion of ethanol to butadiene
- Plackett-Burman design identified key synthesis parameters for high productivity
- TUD-1 synthesis parameters compromised between surface area and pore diameter
- Response Surface Methodology identified high performing catalyst composition

**Abstract:**

The synthesis method of a zinc-tantalum catalyst supported on three-dimensional mesoporous silica with high specific surface area was studied. Its activity in the conversion of ethanol to butadiene was optimized using the Design of Experiment approach. A Plackett-Burman screening design identified the important preparation parameters, notably the ratio of Zn to Ta. It was subsequently optimized using the Response Surface Methodology, affording a highly active catalyst.

**Keywords:** Ethanol; 1,3-Butadiene; TUD-1; Design of Experiment; Supported catalyst

**1. Introduction**

The Lebedev process, the conversion of ethanol to 1,3-butadiene (BD), is being considered as a sustainable alternative to hydrocarbon steam cracking. The latter which currently produces 95% of BD—the world's most consumed diolefin [1–6]. Not only does the Lebedev process use a widely available feedstock derivable from biomass, it is also much more selective towards BD than steam cracking [1]. Selectivity comes into play when considering the purity needed by polymerization catalytic processes used to synthesize rubber from BD [5–7]. However, to financially compete with fossil-based routes, the Lebedev process requires—amongst other things—better performing catalysts [8,9].

Silica-supported metal and metal oxide mixtures have demonstrated high catalytic activity in the Lebedev process [1,4]. Their performances are owed to the multi-functionality provided by the

combination of different metals or metal oxides, each possessing complementary chemical properties required to catalyze the multi-step ethanol-to-butadiene reaction (Fig. 1). A balance between these properties has been cited as the key to maximizing BD production [10]. We found through a preliminary rough screening study (not published) that silica-supported Zn and Ta yielded the largest amount of BD compared with the other transition metals tested, e.g., Al, V, Cu, Ga, Zr, Nb, Hf, La, and Ce. In addition, catalyst structural properties have been linked to superior catalytic activity in the Lebedev process: high active phase dispersion [11–15], large specific surface areas [15,16], three-dimensional mesoporous morphology [8,11,17] were all found to improve catalytic performances in metrics such as BD productivity, BD selectivity and resistance to coke deactivation.

In our previous work, we used the procedure developed at the Delft University of Technology to synthesize mesoporous silica (TUD-1) to prepare a Zn-Ta-TUD-1 catalyst showing remarkable performances in the conversion of ethanol to BD compared to commercial silica and dealuminated BEA materials [18,19]. The Zn-Ta-TUD-1 material proved to be more productive and stable than other highly active catalysts under comparable reaction conditions, notably hierarchical MgO-SiO<sub>2</sub> reported by Men *et al.* and Zn-Y/SiBEA reported by Li *et al.* [20,21]

We seek to improve the performances of the Lebedev process by tuning the synthesis of catalysts possessing the important physical and chemical properties mentioned above. TUD-1 materials have a three-dimensional sponge-like mesoporous morphology and many advantages over conventional mesoporous catalyst carriers [22,23]. They boast a simple, yet cost-effective one-pot synthesis based on the sol-gel process, with tunable pore size and specific surface area, ranging from 2 – 50 nm and 400 – 1000 m<sup>2</sup>/g, respectively. TUD-1 materials are also reported to have a high hydrothermal stability, which suits them well for processes involving the dehydration of alcohol at high temperature. Furthermore, metals are easily introduced and dispersed within the

silica framework with minor adaptation of the preparation procedure [23]. A key component of the TUD-1 synthesis is the addition of an organic chelating agent during the sol-gel process: it forms complexes of the metal and silica precursors, insuring their homogeneous dispersion throughout the preparation by preventing cluster formation; it also acts as a structure-directing agent to produce the sponge-like morphology when the silica precursor condenses during thermal treatment of the gel [23,24]. Catalysts with a highly dispersed active phase, a large specific surface area and a mesoporous morphology for the Lebedev process can thus be obtained. However, despite its simplicity, the TUD-1 preparation procedure needs to be treated carefully: the effects of several synthesis parameters are unclear in the literature, which may cause unexpected result when scientists attempt to adapt the method for their own purposes. Furthermore, authors working with TUD-1 sometimes omit to justify their preferences when adapting the synthesis method. One instance we encountered was the use of tetraethyl ammonium hydroxide (TEAOH) as an alkalizing agent during the sol-gel process. Although described as optional in the original paper by Jansen et al. [18] most scholars resort to it, undoubtedly due to its role as gelation catalyst. However, the quantity in relation to silica precursor amount appears to arbitrarily change from one publication to another [22,25,26]. Parameters we found to change depending on the publication were the calcination method [25,27] and solvent used [22,25,28–30], amongst other.

The objective of our work was thus two-fold: to prepare a Zn-Ta-TUD-1 catalyst active in the Lebedev process based on the observations of our previous work, as well as sorting and understanding the effect of certain synthesis variables on the morphology of bimetallic TUD-1. These goals were achieved using a Design Of Experiment (DOE) methodology combined with mathematical and statistical techniques which allow the modeling of dependent responses to the independent variables of a process. Such models can be used for process optimization, but also for statistical interpretation in order to study the influence exerted by each independent variable on the

selected response. First, a Plackett-Burman (PB) experimental design was used to identify important variables of the Zn-Ta-TUD-1 synthesis and their impact on BD productivity, specific surface area and pore size. It is a two-level factorial design of experiment that allows the screening of  $n - 1$  factors in a maximum of  $n$  experiments, where  $n$  is the number of runs and a multiple of four [31,32]. This highly economical design is ideal for studying processes that are expensive or time-consuming, but comes at the cost of screening resolution, meaning only the main effects of each variables can be calculated. With a better understanding of the Zn-Ta-TUD-1 synthesis, the catalyst was further optimized for BD productivity using a three-level factorial design of experiment combined with the response surface methodology (RSM), a mathematical-statistical technique used in engineering for experiment design and process optimization [31,33–35]. In this case, only two independent variables were selected—Zn and Ta concentration in the catalyst—enabling a more descriptive study of their effect on BD productivity. Catalytic testing and characterization of the morphological properties were performed to gather the experimental data needed for empirical modelling.

## **2. Material and methods**

### **2.1. Reagents & materials**

For the synthesis of Zn-Ta-TUD-1, two sources of each metal were used alternatively: tantalum chloride (Alfa Aesar, 99.8%) or optical grade tantalum ethoxide (Alfa Aesar, 99.95%), and zinc chloride (Acros Organics, 97+%) or zinc acetate dehydrate (Acros Organics, 98+%). Two different chelating agents were used: triethanol amine (or TEAH<sub>3</sub>, Acros Organic, 99+%) or tetraethylene glycol (or TEG, Agros Organics, 99.5%). Tetraethyl orthosilicate, (or TEOS, Agros Organics, 98%) was the silica precursor. Tetraethyl ammonium hydroxide (or TEOH, Aldrich, 35 wt. % in water) was used as the alkalizing agent to catalyze gelation. Ethanol (Aldrich, 99.8%) was used as the solvent for the synthesis and as reactant during catalytic testing.

Thermal treatment of the dried gel was performed in a 35 mL PTFE-lined autoclave from the Parr Instrument Company. Calcination under air flow was done in a quartz tubular reactor and under static air in a muffled oven.

## 2.2. Characterization

Catalyst structures were characterized with nitrogen physisorption experiments at  $-196\text{ }^{\circ}\text{C}$  using a Micromeritics Tristar II instrument. Prior to analysis, 50–200 mg of catalyst were outgassed under vacuum at  $150\text{ }^{\circ}\text{C}$  for 6 hours. Specific surface area ( $S_{BET}$ ) was calculated with the Brunauer–Emmett–Teller (BET) method. The Barret-Joyner-Halenda model was used to calculate the pore diameter ( $D_p$ ) distribution using the desorption isotherm.

Transmission electron microscopy (TEM) was used to characterize the microstructure of selected Zn-Ta-TUD-1 samples with a FEI Tecnai G2 transmission electron microscope operated at 200 kV.

## 2.3. Catalytic testing

Ethanol conversion was performed with a Multi-R<sup>®</sup> apparatus from Teamcat Solutions SAS [36], which is a high-throughput equipment for heterogeneous catalyst screening. Four glass reactors can be used simultaneously, with the gaseous feed being calibrated to ensure an equal inlet flow using a splitter; the reactor outputs were analyzed with an online Agilent 7890 A equipped with an FID detector. An independently controlled valve enables selecting the output of each reactor for analysis.

Catalyst testing was performed at  $350\text{ }^{\circ}\text{C}$  and a pressure of 1 atm. Each catalyst was ground and sieved to 120 mesh granules, 30 mg of which were loaded in glass reactors and kept in place with SiC. To feed the reactors with ethanol, He was used as a carrier gas. It was passed through a bubbler containing  $\geq 99.8\%$  ethanol, set at pressure and temperature to afford vapor concentration of 4.5%

according to the Antoine's law. Weighted hourly space velocity of ethanol ( $WHSV_{EtOH}$ ) was set to  $5.3 \text{ h}^{-1}$  by adjusting the inlet flow and catalyst mass.

Ethanol conversion ( $X$ , %), the selectivity towards each product ( $S_i$ , %), the molar yield of each product ( $Y_i$ , %) and the productivity in butadiene ( $P_{BD}$ ,  $\text{g}_{BD} \cdot \text{g}_{cat}^{-1} \cdot \text{h}^{-1}$ ) were used to describe catalytic activity—equation 1, 2, 3, and 4 respectively, where  $c_i$  represents the number of carbon moles measured for a given compound  $i$ . These values were recorded after 1 hour on stream, after initial stabilization of the reactor output. The carbon balance (CB) for each test was calculated by dividing the sum of carbon moles detected with the molar amount of carbon introduced as ethanol and found to range between 95 – 105 %.

$$X = \frac{c_{EtOH,in} - c_{EtOH,out}}{c_{EtOH,in}} \cdot 100 \quad (1)$$

$$S_i = \frac{c_{i,out}}{c_{EtOH,in} - c_{EtOH,out}} \cdot 100 \quad (2)$$

$$Y_i = X \cdot S_i \quad (3)$$

$$P_{BD} = X \cdot S_{BD} \cdot WSHV_{EtOH} \cdot 0.587/100 \quad (4)$$

#### 2.4. General Zn-Ta-TUD-1 synthesis

The default TUD-1 preparation method was inspired by the work of Pescarmona et al. [29,37,38]. However, we substituted 2-propanol—the original solvent—by ethanol as the former failed to adequately dissolve some metal precursors. In a typical synthesis (see **Error! Reference source not found.**), 1.741 g of TEOS and the metal precursors, i.e. 0.067 g of  $\text{TaCl}_5$  and 0.257 g of  $\text{Zn Zn}(\text{NO}_3)_2 \cdot 6\text{H}_2\text{O}$ , were added to 30 mL of ethanol under vigorous stirring at room temperature. After obtaining a clear solution, the chelating agent was added dropwise while stirring; if  $\text{TEAH}_3$  was used, it was first dissolved in water with 1:11 molar ratio; a typical synthesis used 1.741 g of  $\text{TEAH}_3$ . The mixture was left to stir for 1 hour, resulting in a clear solution.  $\text{TEAOH}$ ,



35 wt.% in water (i.e. 1.767 g of it) was added dropwise to the clear solution under vigorous stirring. During this step, the solution quickly became white and opaque, before returning to a clear, colorless solution, which was further stirred for 2 hours. This sol was left to age for 24 hours, resulting in gelation. The obtained gel was dried overnight at 100 °C, resulting in a solid, transparent xerogel with varying shades of dark orange. It was gently ground to a fine powder and placed in a Teflon-lined autoclave for a thermal treatment at 180 °C during 6 to 48 hours. The ensuing solid—a sticky powder reminiscent of brown sugar—was calcined at 600 °C for 10 hours.

### 2.5. Plackett-Burman screening study

XLstat, an add-on for the Microsoft Excel<sup>®</sup> software, was used to generate the Plackett-Burman design used for studying the effects of the synthesis parameters on the properties and activity of Zn-Ta-TUD-1 and analyze the responses obtained experimentally (Table 1). XLstat can model the effect of each parameter (also known as variable or factor) of a given response by fitting a first-order polynomial function of the studied parameters (equation 5) with the experimental response.

$$Y_j = \beta_0 + \sum_{i=1}^k \beta_i \cdot X_i + \varepsilon \quad (5)$$

where  $Y_j$  is the fitted response,  $\beta_0$  the model intercept,  $\beta_i$  is the linear coefficient of independent variable  $i$  with  $X_i$  its level,  $k$  the number of involved variables, and  $\varepsilon$  the residual error. Equation 5 was solved using the least square method, which is a multiple regression technique that fits mathematical models to experimental data by minimizing the value of residuals between experimental and fitted responses. Quality of fit and model significance were established by the coefficient of determination ( $R^2$ ) and Fischer's F-test, respectively. The obtained statistical results showed the medialization to be statistically acceptable for further study.

The effect of each variable was judged according to their statistical significance, which was assessed with an analysis of variance (ANOVA) performed with XLstat. For each response, this

required transforming three of the eleven variables into ‘dummy’ variables to reach the minimum variable-to-observation ratio required for statistical analysis. Variables were considered ‘dummy’ when the contribution of their coefficient to the response model was less than 1%. The ANOVA afforded standardized main effects of variables, which are t-statistics that test the null hypothesis, e.g., that the effect of a variable on the response is 0.

BD productivity ( $Y_{BD}$ ) was chosen as the first response to model due to its industrial importance [2,39]. BET specific surface ( $Y_{SBET}$ ) and average pore diameter ( $Y_{Dp}$ ) were selected as responses due to their importance as morphological properties of catalyst carriers. The choice of synthesis variables was based on the literature concerning both the Lebedev process and TUD-1 catalysts, as well as preliminary experiments (not shown). The Zn-to-Ta (Zn:Ta) and total Si-to-metal molar ratios (Si:M) in the precursor gel were selected due to the reported importance of balanced active phases in catalysts for the Lebedev process [10,13,16,40–42]. The nature of the metal precursors, was reported as influential on TUD-1 morphology [22], but also on activity in the Lebedev process.[43] In this case, zinc chloride and zinc acetate hydrate were selected as levels for the zinc precursor parameter (ZnPr). Tantalum chloride and tantalum ethoxide were chosen as tantalum precursors (TaPr). Thermal treatment (ThTr) duration is reported as an important TUD-1 synthesis parameter because of its influence on morphology [23–25]. The TEAOH-to-Si mole ratio in the precursor gel (Alk:Si), the type of chelating agent (ChAg) and the choice of calcination method (CalcM) were selected due to the ambiguity in the literature regarding their influence. For instance, TEAOH is described as optional [18], yet is used in most publications, without an optimal ratio being reported [22,25,26]. The calcination temperature ramp (CalcR) and the need for a drop-wise addition of TEAOH under vigorous stirring (StiDW) were investigated as potential time-saving measures. The order by which the chelating agent was added to the precursor solution (ChOrd) with regards to the metal precursor was also investigated out of curiosity. Fig. 2 illustrates the Zn-

Ta-TUD-1 synthesis methods used in the PB experiment, as well as the different levels of all parameters with the exception Zn:Ta and Alk:Si.

Choosing the two levels of each factor, represented by + and – in Table 1, was largely a matter of preliminary experimentation with the TUD-1 and the result of our unpublished screening study previously mentioned. Table 2 lists the levels of each variable investigated in the Zn-Ta-TUD-1 synthesis; Fig. 2 illustrates these levels in relation to the Zn-Ta-TUD-1 preparation procedure. Experiments were performed in a random order generated by the XLstat software to minimize errors and biases.

## 2.6. Response surface methodology

RSM is a technique that encompasses multi-variant experimental design, statistical modelling and process optimization. It is generally performed in three steps: (1) DOE, (2) response surface modelling through regression and (3) optimization of the response [44]. The XLstat software was used for all three steps. RSM was used to optimize the productivity in BD ( $Y_{PDB}$ ) by establishing its relationship to two independent variables: Zn and Ta molar content in Zn-Ta-TUD-1, Zn mol.% and Ta mol.% respectively. The variables were selected after the PB screening study showed that the Zn:Ta molar ratio had a significant effect on the activity of the catalyst. In addition, the Zn-Ta-TUD-1 preparation method used corresponded to the best performing procedure identified by screening, which was equivalent to that used for sample PB12 in Table 1.

For a single-response, two-variable experiment, a three-level full factorial design was found suitable, as it did not require many experiments, yet provided a reasonable amount of information [35]. The three levels used were symbolized by -1, 0, 1. Table 3 lists the experimental design, the corresponding experimental values for each level and the YPBD response obtained via catalytic testing. Like above, experiments were performed in random order to minimize errors and biases via the XLstat software.

Response surface modelling was performed by an empirical quadratic model of the response (Equation 6) to the experimental data using the least square root method.

$$Y_j = \beta_0 + \sum_{i=1}^k \beta_i \cdot x_i + \sum_{i=1}^k \beta_{ii} \cdot x_i^2 + \sum_{i<j}^k \beta_{ij} \cdot x_i \cdot x_j + \varepsilon \quad (6)$$

where  $Y_j$  is the fitted response,  $\beta_0$  the model intercept,  $\beta_i$  is the linear coefficient of independent variable  $i$  with  $x_i$  its input factor, and  $k$  the number of involved variables,  $\beta_{ii}$  is the quadratic coefficient of variable  $i$ ,  $\beta_{ij}$  is the linear interaction coefficient between variable  $i$  and  $j$ , and  $\varepsilon$  the residual error. Goodness of fit of the model was evaluated with  $R^2$  and its significance with Fischer's F-test. Contrarily to the modelling used in the PB experiment, the introduction of second-order terms allows the study of variable interaction effects. The relevance of each coefficient was judged according to the t-statistics resulting from an ANOVA.

Optimization, e.g., finding the variable level providing the theoretical maximum response, was performed using the method of steepest ascent, which is available due to the model being limited to a single response [31].

### 3. Results and discussion

#### 3.1. Plackett-Burman screening

##### 3.1.1. Statistical interpretation

The coded value of experimental points representing the variables of the Zn-Ta-TUD-1 synthesis and the corresponding responses are listed in Table 1. For each response—BD productivity, BET surface area and average pore diameter—a first-order polynomial equation was generated and fitted to the experimental data. Accuracy of fit and F-test results (**Error! Reference source not found.**) indicate that all three models explain >94% of the response variation and are overall significant at 95% confidence level. An association test of the studied responses with

Pearson-type correlation was performed at 95% confidence level. The correlation matrix can be found in Table 4.

The calculated linear coefficient  $\beta_i$  of every independent variable  $i$  can be used to estimate their influence on each response. A more rigorous interpretation considers the standardized main effects, which are the t-values of variable effects computed with the ANOVA of the models [32]. Two criteria were used to judge the importance of each variable: the t-value limit at confidence level of 95% ( $\alpha = 0.05$ ) and the Bonferroni limit, which tests the null hypothesis at more conservative confidence level [32]. Factors with standardized effects above the t-value limit were interpreted as likely to be significant; above the Bonferroni limit, variables were considered significant [32,45]. Below the t-value limit, variables were deemed unlikely to be significant.

Pareto charts of standardized effects are simple bar charts, but a useful visualization tool to quickly interpret the results of factorial screening studies through. By plotting the t-value and Bonferroni limits, the significant of each variable of the Zn-Ta-TUD-1 synthesis can be easily assessed. The length of each bar also indicates the relative weight of each variable. The effects each experimental level of the synthesis parameters had on the responses were also considered. For a given response, dashed bars indicate that the low level (-) of the parameter afforded the greater response value comparatively. Contrarily, dash-less bars indicate that the high level (+) gave a higher response. Pareto charts of standardized effects of Zn-Ta-TUD-1 synthesis on BD productivity,  $S_{BET}$  and  $D_p$  are illustrated in Fig. 3.

### 3.1.2. Zn-Ta-TUD-1 morphology

The results of  $N_2$  porosimetry with the catalysts prepared according to the PB design are listed in Table 1. These confirm the formation of mesoporous materials with high surface area. As Table 1 indicates, BET specific surface area ( $Y_{BET}$ ) ranged between 228 and 747  $m^2g^{-1}$  and average pore

diameter ( $Y_{Dp}$ ) varied between 3.0 and 25.1 nm. This degree of irregularity in terms of morphological properties is consistent with the high tunability of TUD-1 materials.

In the original paper introducing the TUD-1 synthesis procedure, Jansen *et al.* explained how the mesoporous morphology could be tuned [18]. By adjusting the thermal treatment duration of the silica xerogel, pore diameter and specific surface area could be modified, with the value of each characteristic being inversely proportional to one another as a function of time—lengthening treatment time reducing specific surface area and increasing mesopore size. Similar observations were made with metal-containing TUD-1 materials when time was the only synthesis variable [24].

The xerogel is an organic-inorganic hybrid in which the chelating agent and its metal complexes are homogeneously dispersed [24]. Upon heating, silica particles grow and organic species agglomerate, shaping the mesoporous framework by steric hindrance. In theory, lengthening the heating period promotes the organic agglomeration [46], resulting in larger, but fewer agglomerates for silica to condense around. The morphological consequence of this phenomenon is larger pores, but a reduced specific surface area. This trade-off between the two morphological properties as a result of thermal treatment time is well established [18,23,46].

Surprisingly, the statistical analysis of the effects exerted by the 11 variables of the Zn-Ta-TUD-1 synthesis under study (Fig. 3) found thermal treatment time not to influence BET specific surface area or the average mesopore size. Nevertheless, the association test (Table 4) indicated a strong inverse correlation between the two morphological properties. In other words, the trade-off between surface area and pore size typical of TUD-1 still took place, but was the subject of variables other than thermal treatment time. Fig. 5 illustrates this relationship. The type of chelating agent and TEAOH:Si ratio in the precursor gel were identified as statistically significant variables influencing both morphological properties. According to the literature, TEAH<sub>3</sub> and TEG play the identical dual role of precursor chelating and structure directing agents, with the former being the

predominant choice in TUD-1 synthesis.[23] However, no study could be found that directly compared both molecules. Interestingly, TEG led to larger specific surface area and TEAH<sub>3</sub> to larger pores. This is consistent with the fact the latter has a larger molar volume than TEG, both when determined empirically at 25 °C and using Connolly's molecular surface package [47], since equimolar amounts were used in the synthesis of Zn-Ta-TUD-1. Incidentally, greater quantities of TEAOH—used for catalyzing the gelation process and introduce micropores within the framework—was correlated with bigger pore diameter at the expense of surface area, although no micropores could be detected by N<sub>2</sub> porosimetry. The additional organic matter within the precursor gel likely increases the size of structure-shaping agglomerates during the thermal treatment. Consequently, the use of TEOH should be limited to gelation catalysis, as its structure-directing properties could be fulfilled by the less expensive, safer chelating agents.

Other synthesis variable studied showed significant effect on the morphological properties of Zn-Ta-TUD-1 (Fig. 3). However, these were not reciprocal between both responses studied. Considering the inverse correlation observed, two possibilities main explain this discrepancy: these variables exclusively affected one of the morphological properties independently of the other; interaction effects between variables also influencing TUD-1 morphology could not be estimated due to the low degree of freedom of PB designs [31]. The most important synthesis parameter identified to only affect pore size was the TEAOH addition procedure during the sol-gel process. Most authors indicate TUD-1 should be prepared by adding TEAOH drop-wise under vigorous stirring and left stirring for up to two hours until a clear gel is obtained. Surprisingly, directly pouring TEOH consistently afforded a clear colorless gel, whereas the traditional method occasionally resulted in milky mixtures, which have been observed elsewhere.[26,46] In the sol-gel methodology, the basic catalyst feed rate controls the silica precursor hydrolysis and condensation kinetics; higher feed rates have been associated to faster particle growth.[48]

Consequently, the influence of the TEAOH addition method on the morphology of Zn-Ta-TUD-1 may be owed to the change in gelation kinetics it induces. Why this effect is statistically significant only for the average pore diameter remains to be answered.

### 3.1.3. BD productivity

The catalytic performances of Zn-Ta-TUD-1 catalysts prepared according to PB design varied significantly in terms of productivity (Table 3). In a typical test, ethanol was converted to predominantly three products: BD, acetaldehyde and ethylene; 1–3 % yield consisted of diethyl ether, propylene, 1-butanol and butenes. Selectivity towards the three main products depended on the catalyst used. The best performances were achieved with PB12: its activity is depicted in Fig. 4. As illustrated, BD selectivity reached 70%, a value comparable to many of the best catalysts found in the literature [4]. Although BD selectivity remained stable, deactivation took place, as evidenced by the decreasing ethanol conversion. Nevertheless, high BD productivity was achieved.

As previously indicated, several authors have associated the morphology of studied materials and their performances in the Lebedev process [8,11,16,17]. Association tests of BD productivity with specific surface area and average pore diameter were performed. Accordingly, a Pearson-type correlation between BD productivity and specific surface area at 95% confidence interval was found (Table 4); although statistically significant, it is unlikely that the correlation is linear, as a better fit was found with a quadratic equation (Fig. 5 (b)). Similar correlations have been reported by other scholars for this reaction [16]. In fact, it is well-established that greater surface area allows for a better accessibility to active sites and is often considered a desirable feature of catalysts. Contrarily to Jones et al. [8] and Palkovits et al. [17], who reported improvements in BD yield with increasing pore size, no correlation could be found between the average pore diameter and BD productivity on Zn-Ta-TUD-1. This can be explained by the trade-off between  $S_{\text{BET}}$  and  $D_p$  mentioned in section 3.1.2.: the benefits of greater pore size may be cancelled due to the loss in



specific surface area, suggesting the latter to be the most important morphological property of the two for maximization BD formation. Consequently, it is unsurprising that two of the most influential factors on  $S_{BET}$ , the nature of the chelating agent and the calcination method, were also statistically significant on BD productivity, as depicted by Fig. 3 (c).

The only factor with no impact on TUD-1 morphology, but significantly influential on BD productivity was the Zn-to-Ta molar ratio. Zinc oxide is well-established for catalyzing the dehydrogenation of ethanol and tantalum oxide can perform the conversion of ethanol-acetaldehyde mixtures of BD. However, many authors have reported that a subtle balance must be struck between the dehydrogenating and condensation promoters, as the active sites are also known to catalyze undesirable side-reaction. This theory is given statistical evidence through the results of our PB screening. The fact that the Zn-to-Ta molar ratio was statistically insignificant on synthesis procedure with regards to the resulting morphological properties further indicates that it is solely attributable to the chemical properties of Zn-Ta-TUD-1.

Further increase in BD productivity proceeded by tuning the synthesis of Zn-Ta-TUD-1. Of all significant preparation parameters identified by the PB design experiment, the Zn-to-Ta ratio was selected for the RSM experiment. To accommodate a two-variable design, Zn-to-Ta was split into the molar amount of each element, thereby providing information of the effect of low metal content. All other variables were set to their low-level setting, as Fig. 3 shows them to improve BD productivity. Incidentally, this corresponds to the procedure used to synthesize PB12, except for the ratio and amount of Zn and Ta.

## **3.2. Response surface methodology**

### **3.2.1 Statistical interpretation**

The obtained response listed in Table 3 was correlated with independent variables Zn mol.% and Ta mol.% using the quadratic equation, Eq. (6). The least square regression method was used to fit the experimental data to Eq. (6), resulting in the model below:

$$Y_{PBD} = 1.191 + 0.146 \cdot X_1 + 0.156 \cdot X_2 + 0.059 \cdot X_1^2 - 0.366 \cdot X_2^2 - 0.031 \cdot X_1 \cdot X_2 \quad (7)$$

where  $X_1$  is Zn mol.% and  $X_2$  is Ta mol.%. Validity of the model was tested through statistical means (**Error! Reference source not found.****Error! Reference source not found.**). The coefficient of determination and its adjusted form, 0.971 and 0.924, respectively, showed that the experimental results were well represented by the model. ANOVA of the model indicated an F-value of 20.347 and a p-value below 0.05; these statistical results demonstrated the significance and adequacy of the model.

The importance of each factor on the response (BD productivity) was assessed by comparing their standardized effect to the minimum t-value at 95% confidence interval. The Pareto chart depicted in Fig. 6 reveal the most important factors. The main effect of Zn and Ta content were found to be important, naturally suggesting both elements contribute to the catalytic activity of Zn-Ta-TUD-1. However, no interaction effect could be discerned between the two variables; this implies Zn and Ta—although both required for forming BD—do not have a synergy effect that can be discerned using our quadratic model. Only the squared effect of Ta loading was significant, but also negative. This can be interpreted as a non-linear detrimental effect of Ta mol.% on BD productivity.

The two-dimensional contour plot of BD productivity corroborated with Zn and Ta loadings is shown in Fig. 7; it is the visual representation of the quadratic response model, Eq. 7. A noticeable plateau effect with regards to the Ta loading can be deduced from its shape [35], reflecting the squared negative effect noted above. A linear relation between BD productivity with Zn content

within the experimental region can also be observed. The method of steepest ascent indicated BD productivity can be maximized with a catalyst containing 3 mol.% of Zn and 2.2 mol.% of Ta. However, the elliptical shape of the response maxima suggests the true optimal value to be outside the experimental region with regards to Zn content. Incidentally, PB12—synthesized for the screening experiment with a loading of 4 mol.% Zn and 2.1 mol.% Ta—showed a BD productivity of  $1.60 \text{ g}_{\text{BD}} \cdot \text{g}_{\text{cat}}^{-1} \cdot \text{h}^{-1}$ . A Zn-Ta-TUD-1 catalyst with 6 mol.% and 2.2 mol.% of Zn and Ta was synthesized using the same methodology to further test the influence of Zn. BD productivity dropped to  $0.86 \text{ g}_{\text{BD}} \cdot \text{g}_{\text{cat}}^{-1} \cdot \text{h}^{-1}$ , with a noticeable gain in acetaldehyde selectivity (not shown). The resulting curve of PB selectivity versus Zn mol.% at fixed Ta content the RSM indicated the optimal Zn-Ta-TUD-1 catalyst should have a Zn content between 3 and 4 mol.%. Ta content between 2 and 2.2 mol.% was found optimal with the method of steepest ascent. This amounts to a Zn-to-Ta ratio between 1.5 and 2.

### 3.2.2. RSM series characterization

The TUD-1 preparation has been described as an easy way to homogeneously disperse metals within a mesoporous silica framework [23]. Optimization of Zn-Ta-TUD-1 synthesis to maximize its activity in the Lebedev process afforded highly active materials. To verify that the materials prepared were comparable to those found in the literature, thereby confirming the success of the synthesis method used, characterization was performed.

$\text{N}_2$  porosimetry results (Table S3) indicated the final Zn-Ta-TUD-1 method afforded materials with an average BET surface area of  $661 \pm 41 \text{ m}^2 \cdot \text{g}^{-1}$ , indicative of its repeatability. Average pore size diameter of  $9.8 \pm 1.5 \text{ nm}$  was obtained, with an outlier at 7.0 nm. Interestingly, no correlation between BET surface area and activity could be observed. This suggested the metal content becomes the predominant factor once specific area is large enough, e.g.,  $\geq 600 \text{ m}^2 \cdot \text{g}^{-1}$  at which point this morphological property appears to no longer be an issue.

SEM images typical of samples prepared during the RSM experiments are shown in Fig. 8. The results are similar to those reported in the literature for M-TUD-1 at low metal loading [25,30,38,49–51]. Zn-Ta-TUD-1 consisted of  $<100\ \mu\text{m}$  particles apparently without a well-defined morphology. At high magnification, the catalyst surface is shown to be rough and irregular, typical of the sponge-like morphology resulting from the agglomeration of silica particles formed during the synthesis procedure [23,24,52].

Fig. 9 illustrates HR-TEM images of RSM series Zn-Ta-TUD-1 catalysts. Inspection of various samples confirmed the sponge-like 3D structure with “worm-like” pores characteristic of TUD-1 materials [23,26]. The absence of discernable metal oxide nanoparticles suggests Zn and Ta were completely isolated within the carrier framework. Their presence was confirmed by energy-dispersive X-ray spectroscopy. Furthermore, nanoparticles could be detected upon electron irradiation of the samples, which provoked the degradation of silica and metal oxide agglomeration (Fig. 9, right, and **Error! Reference source not found.**) [53,54].

### 3 Conclusion

The effect of various parameters in the synthesis of Zn-Ta-TUD-1 materials on their morphology and ability to convert ethanol to BD was studied using designs of experiments. A Plackett-Burman screening design coupled with mathematical modelling and statistical tools identified the most important preparation variables for attaining high BD productivity and understanding their effect on surface area and pore size. Response surface methodology was used to optimize BD productivity by tuning the Zn and Ta content of catalysts prepared according to the most suitable procedure resulting from the screening study.

We found the nature of the chelating agent to play a statistically significant role on the morphology of Zn-Ta-TUD-1. Use of TEG—a sterically smaller molecule—resulted in larger surface area and smaller average pore diameter than TEAH<sub>3</sub>. There existed a trade-off situation

between the two structural properties depending on the agent used and the total amount of organic species present in the precursor gel. Ostensibly, the difference manifests itself during the structure shaping process taking place under thermal treatment. Choosing a favorable chelating agent may be an alternative to tuning the thermal treatment duration for obtaining desirable morphologies, the common practice with TUD-1 material. New chelating agents and their effect should also be investigated.

Substituting the drop-wise addition under stirring of TEAOH for rapid pouring influenced pore size, likely due to changes in the gelation kinetics. It showed great reproducibility in obtaining materials with large surface area ( $\geq 600 \text{ m}^2 \cdot \text{g}^{-1}$ ) and mesopores diameters averaging 10.5 nm. In practical terms, this finding enables time saving during the synthesis. However, a more thorough study of the gelation kinetics with better controlled alkalizing agents addition rates is advised.

Besides the chelating agent, high BD productivity required a balanced Zn:Ta ratio and calcination of the samples under air. RSM optimization of Zn and Ta loadings further indicated the optimal content of Ta was between 2 and 2.2 mol.%. Maximum BD productivity required a Zn content between 3 and 4 mol.%. Despite finding no mathematical evidence of interaction between the amount of Zn and Ta, the results highlight the need for a balanced quantity of each element for maximizing BD production. This observation coincides with other findings of the literature which concluded that the multi-step reaction of the Lebedev process requires catalysts with balanced properties, often obtaining by tuning their different components [10,16,40].

The butadiene productivity of catalyst RSM-8 prepared *via* the improved synthesis method can be compared with that Zn-Ta-TUD-1 from our previous work—synthesized by conventional method with unoptimized metal content [19]. At 400 °C and  $\text{WHSV}_{\text{EtOH}}$  of  $5.3 \text{ h}^{-1}$ , RMS-8 achieves a comparable BD productivity of  $2.18 \text{ g}_{\text{BD}} \cdot \text{g}_{\text{cat}}^{-1} \cdot \text{h}^{-1}$  after 3 hours on stream, despite possessing 53% of the total metal content (3 and 2 mol.% *vs.* 6.1 and 3.4 mol% of Zn and Ta, respectively).

Furthermore, RSM-8 displayed a better resistance to deactivation over a 20 h period, decreasing by 8 percentage points, compared to 16 percentage points for the catalyst of our previous work (Fig. S3). Consequently, we conclude that the design of experiment approach successfully improved the synthesis method for preparing Zn-Ta-TUD-1 materials highly active in the Lebedev process.

**Guillaume Pomalaza:** Investigation, Methodology, Formal analysis, Writing – Original Draft. **Mickaël Capron:** Supervision, Funding Acquisition. **Franck Dumeignil:** Supervision, Writing – Review & Editing, Funding Acquisition, Validation.

#### 4 Acknowledgements

Authors acknowledge the support from the French National Research Agency (ANR-15-CE07-0018-01). Chevreul Institute (FR 2638), Ministère de l'Enseignement Supérieur, de la Recherche et de l'Innovation, Région Hauts-de-France and FEDER are acknowledged for supporting and funding partially this work.

## References

- [1] E. V Makshina, M. Dusselier, W. Janssens, J. Degève, P.A. Jacobs, B.F. Sels, *Chem. Soc. Rev.* 43 (2014) 7917–7953.
- [2] D. Cespi, F. Passarini, I. Vassura, F. Cavani, *Green Chem.* 18 (2016) 1625–1638.
- [3] S. Farzad, M.A. Mandegari, J.F. Görgens, *Bioresour. Technol.* 239 (2017) 37–48.
- [4] G. Pomalaza, M. Capron, V. Ordonsky, F. Dumeignil, *Catalysts* 6 (2016) 203.
- [5] H.N. Sun, J.P. Wristers, in: *Kirk-Othmer Encycl. Chem. Technol.*, John Wiley & Sons, Inc., Hoboken, NJ, USA, 2002.
- [6] M. Dahlmann, J. Grub, E. Löser, in: *Ullmann's Encycl. Ind. Chem.*, Wiley-VCH Verlag GmbH & Co. KGaA, Weinheim, Germany, 2011, pp. 1–24.
- [7] C. Angelici, M.E.Z. Velthoen, B.M. Weckhuysen, P.C.A. Bruijninx, *ChemSusChem* 7 (2014) 2505–2515.
- [8] M. Jones, C. Keir, C. Iulio, R. Robertson, C. Williams, D. Apperley, *Catal. Sci. Technol.* 1 (2011) 267.
- [9] G.O. Ezinkwo, V.P. Tretyakov, A. Aliyu, A.M. Ilolov, *ChemBioEng Rev.* 1 (2014) 194–203.
- [10] C. Angelici, M.E.Z. Velthoen, B.M. Weckhuysen, P.C.A. Bruijninx, *Catal. Sci. Technol.* 5 (2015) 2869–2879.
- [11] T.W. Kim, J.W. Kim, S.Y. Kim, H.J. Chae, J.R. Kim, S.Y. Jeong, C.U. Kim, *Chem. Eng. J.* 278 (2014) 217–223.
- [12] J.L. Cheong, Y. Shao, S.J.R. Tan, X. Li, Y. Zhang, S.S. Lee, *ACS Sustain. Chem. Eng.* 4 (2016) 4887–4894.
- [13] V.L. Sushkevich, I.I. Ivanova, V. V. Ordonsky, E. Taarning, *ChemSusChem* (2014) 2527–

2536.

- [14] A. Tripathi, K. Faungnawakij, A. Laobuthee, S. Assabumrungrat, N. Laosiripojna, *Int. J. Chem. React. Eng.* 14 (2016) 945–954.
- [15] V.L. Dagle, M.D. Flake, T.L. Lemmon, J.S. Lopez, L. Kovarik, R.A. Dagle, *Appl. Catal. B Environ.* 236 (2018) 576–587.
- [16] S. Da Ros, M.D. Jones, D. Mattia, J.C. Pinto, M. Schwaab, F.B. Noronha, S.A. Kondrat, T.C. Clarke, S.H. Taylor, *ChemCatChem* 8 (2016) 2376–2386.
- [17] A. Klein, R. Palkovits, *Catal. Commun.* 91 (2016) 72–75.
- [18] J.C. Jansen, Z. Shan, L. Marchese, W. Zhou, N. v d Puil, T. Maschmeyer, *Chem. Commun.* (2001) 713–714.
- [19] G. Pomalaza, G. Vofo, M. Capron, F. Dumeignil, *Green Chem.* 20 (2018) 3203–3209.
- [20] X. Huang, Y. Men, J. Wang, W. An, Y. Wang, *Catal. Sci. Technol.* 7 (2017) 168–180.
- [21] W. Dai, S. Zhang, Z. Yu, T. Yan, G. Wu, N. Guan, L. Li, *ACS Catal.* 7 (2017) 3703–3706.
- [22] A. Ramanathan, M. Carmen Castro Villalobos, C. Kwakernaak, S. Telalovic, U. Hanefeld, *Chem. - A Eur. J.* 14 (2008) 961–972.
- [23] S. Telalović, A. Ramanathan, G. Mul, U. Hanefeld, *J. Mater. Chem.* 20 (2010) 642.
- [24] M.S.H.M. Saad, *Functionalized TUD-1 : Synthesis , Characterization and (Photo-) Catalytic Performance*, Universiteit Van Hewan, 2005.
- [25] S. Lima, M.M. Antunes, A. Fernandes, M. Pillinger, M.F. Ribeiro, A.A. Valente, *Molecules* 15 (2010) 3863–3877.
- [26] A. Ranoux, K. Djanashvili, I.W.C.E. Arends, U. Hanefeld, *RSC Adv.* 3 (2013) 21524–21534.
- [27] G. Imran, M.P. Pachamuthu, R. Maheswari, A. Ramanathan, S.J. Sardhar Basha, *J. Porous Mater.* 19 (2012) 677–682.
- [28] B. Karmakar, A. Sinhamahapatra, A.B. Panda, J. Banerji, B. Chowdhury, *Appl. Catal. A*



- Gen. 392 (2011) 111–117.
- [29] L. Li, D. Cani, P.P. Pescarmona, *Inorganica Chim. Acta* 431 (2015) 289–296.
- [30] M.S. Hamdy, O. Berg, J.C. Jansen, T. Maschmeyer, J.A. Moulijn, G. Mul, *Chem. - A Eur. J.* 12 (2006) 620–628.
- [31] M. Natrella, NIST/SEMATECH e-Handbook of Statistical Methods, NIST/SEMATECH, 2010.
- [32] J. Madinger, P.J. Whitcomb, *DOE Simplified*, Productivity Press, 2017.
- [33] M. Zougagh, P.C. Rudner, A.G. De Torres, J.M. Cano Pavôn, *J. Anal. At. Spectrom.* 15 (2000) 1589–1594.
- [34] T. Lundstedt, E. Seifert, L. Abramo, B. Thelin, Å. Nyström, J. Pettersen, R. Bergman, *Chemom. Intell. Lab. Syst.* 42 (1998) 3–40.
- [35] M.A. Bezerra, R.E. Santelli, E.P. Oliveira, L.S. Villar, L.A. Escaleira, *Talanta* 76 (2008) 965–977.
- [36] F. Dumeignil, S. PAUL, L. Duhamel, J. FAYE, P. Miquel, M. CAPRON, J.L. Dubois, Dispositif d'évaluation d'au Moins Un Critère de Performance de Catalyseurs Hétérogènes, WO2015118263 A1, 2015.
- [37] L. Li, T.I. Korányi, B.F. Sels, P.P. Pescarmona, *Green Chem.* 14 (2012) 1611.
- [38] I.C. Neves, G. Botelho, A. V. Machado, P. Rebelo, S. Ramôa, M.F.R. Pereira, A. Ramanathan, P. Pescarmona, *Polym. Degrad. Stab.* 92 (2007) 1513–1519.
- [39] E. V. Makshina, W. Janssens, B.F. Sels, P.A. Jacobs, *Catal. Today* 198 (2012) 338–344.
- [40] S.-H. Chung, C. Angelici, S.O.M. Hinterding, M. Weingarth, M. Baldus, K. Houben, B.M. Weckhuysen, P.C.A. Bruijninx, *ACS Catal.* 6 (2016) 4034–4045.
- [41] O. V. Larina, P.I. Kyriienko, S.O. Soloviev, *Theor. Exp. Chem.* 52 (2016) 51–56.
- [42] P.I. Kyriienko, O. V. Larina, S.O. Soloviev, S.M. Orlyk, C. Calers, S. Dzwigaj, *ACS Sustain.*

- Chem. Eng. 5 (2017) 2075–2083.
- [43] T. De Baerdemaeker, M. Feyen, U. Müller, B. Yilmaz, F.S. Xiao, W. Zhang, T. Yokoi, X. Bao, H. Gies, D.E. De Vos, ACS Catal. 5 (2015) 3393–3397.
- [44] P.N. Panahi, D. Salari, A. Niaei, S.M. Mousavi, J. Ind. Eng. Chem. 19 (2013) 1793–1799.
- [45] A. Hesari, P. Mohammad, A.H. Fererdoon, A. Mehdi, Iran. J. Chem. Chem. Eng. 35 (2016) 51–62.
- [46] Z. Shan, J.C. Jansen, W. Zhou, T. Maschmeyer, Appl. Catal. A Gen. 254 (2003) 339–343.
- [47] M.L. Connolly, M.P.W. Shell, 11 (1993) 139–141.
- [48] I.A. Rahman, P. Vejayakumaran, C.S. Sipaut, J. Ismail, M.A. Bakar, R. Adnan, C.K. Chee, Colloids Surfaces A Physicochem. Eng. Asp. 294 (2007) 102–110.
- [49] M.P. Pachamuthu, V.V. Srinivasan, R. Maheswari, K. Shanthi, A. Ramanathan, Appl. Catal. A Gen. 462–463 (2013) 143–149.
- [50] W. Yan, A. Ramanathan, P.D. Patel, S.K. Maiti, B.B. Laird, W.H. Thompson, B. Subramaniam, J. Catal. 336 (2016) 75–84.
- [51] M.P. Pachamuthu, K. Shanthi, R. Luque, A. Ramanathan, Green Chem. 15 (2013) 2158.
- [52] A. Ranoux, K. Djanashvili, I.W.C.E. Arends, U. Hanefeld, RSC Adv. 3 (2013) 21524.
- [53] N. Jiang, Reports Prog. Phys. 79 (2016) 016501.
- [54] B. Martin, O.W. Flörke, E. Kainka, R. Wirth, Phys. Chem. Miner. 23 (1996) 409–417.

## 5 ANNEX - FIGURES

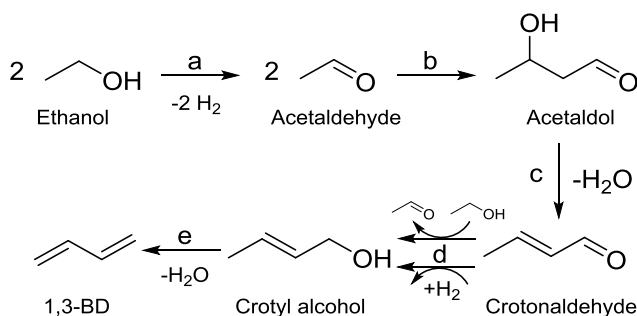


Fig. 1 Generally accepted mechanism for the conversion of ethanol to 1,3-butadiene. Reaction steps: (a) ethanol dehydrogenation; (b) aldol condensation of acetaldehyde; (c) acetaldol

Table 1 Plackett-Burman experimental design used for studying the main effects of Zn-Ta-TUD-1 synthesis variables.

Run no.	Cat. name	Variable											Responses		
		Zn:Ta	Si:M	ThTr	TaPr	ZnPr	ChAg	Alk:Si	ChOrd	StiDW	CalcM	CalcR	$Y_{PBD}$	$Y_{SBET}$	$Y_{DP}$
1	PB1	+	+	-	+	+	+	-	-	-	+	-	0.583	341	18.7
10	PB2	-	+	+	-	+	+	+	-	-	-	+	1.089	336	25.3
11	PB3	+	-	+	+	-	+	+	+	-	-	-	0.644	424	28.3
2	PB4	-	+	-	+	+	-	+	+	+	-	-	1.139	747	3
6	PB5	-	-	+	-	+	+	-	+	+	+	-	0.748	516	7
4	PB6	-	-	-	+	-	+	+	-	+	+	+	0.753	228	25.11
5	PB7	+	-	-	-	+	-	+	+	-	+	+	0.669	401	26
3	PB8	+	+	-	-	-	+	-	+	+	-	+	0.745	505	15.9
7	PB9	+	+	+	-	-	-	+	-	+	+	-	0.640	486	12.6
8	PB10	-	+	+	+	-	-	-	+	-	+	+	0.912	601	11.9
9	PB11	+	-	+	+	+	-	-	-	+	-	+	1.181	740	6.6
12	PB12	-	-	-	-	-	-	-	-	-	-	-	1.602	739	10.7

Variable signification: Zn:Ta, the zinc-to-tantalum molar ratio; Si:M, the silica-to-total-metal ratio; ThTr, the thermal treatment time; TaPr, nature of the Ta precursor; ZnPr, nature of the Zn precursor; ChAg, nature of the chelating agent; Alk:Si, the TEAOH-to-Si ratio; ChOrd, the order of chelation; StiDW, Dropwise addition of TEAOH with stirring; CalcM, calcination method; CalcR, calcination ramp.

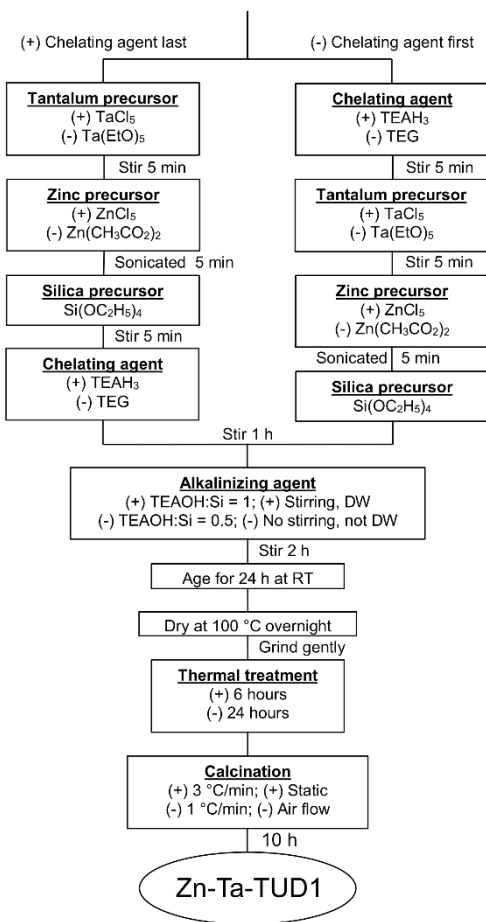


Fig. 2 Preparation scheme of Zn-Ta-TUD-1; (+) and (-) signs represent the levels of the Plackett-Burman experimental design.

Table 2 Level of variables in the Plackett-Burman experiment of Zn-Ta-TUD-1 synthesis

Variable	Unit	Symbol	-	+
Zn-to-Ta ratio	n/a	Zn:Ta	2	5
Silica-to-metal ratio	n/a	Si:M	16	8
Thermal treatment duration	Hour	ThTr	6	24
Nature of Ta precursor	n/a	TaPr	Ta(EtO) <sub>5</sub>	TaCl <sub>5</sub>
Nature of Zn precursor	n/a	ZnPr	Zn(CH <sub>3</sub> CO <sub>2</sub> ) <sub>2</sub>	ZnCl <sub>5</sub>
Nature of chelating agent	n/a	ChAg	TEG	TEAH <sub>3</sub>
TEAOH-to-Si ratio	n/a	Alk:Si	0.5	1.0
Order of chelation addition step	n/a	ChOrd	Before metal	After metal
Dropwise addition of TEAOH with stirring	n/a	StiDW	No	Yes
Calcination method	n/a	CalcM	Under air flow	Under static air
Calcination temperature ramp	°C/min	CalcR	1	3

Table 3 Three-level factorial design and corresponding levels of variable for the optimization of Zn-Ta-TUD-1 preparation to maximize butadiene productivity and the corresponding experimental responses.

Run no.	Catalyst name	Variable		$Y_{PBD}$ (g <sub>BD</sub> g <sub>cat</sub> <sup>-1</sup> h <sup>-1</sup> )
		Ta mol. %	Zn mol. %	

2	RSM1	-1	1 %	-1	1 %	0.555
5	RSM2	0	2 %	-1	1 %	1.048
4	RSM3	1	3 %	-1	1 %	0.978
9	RSM4	-1	1 %	0	2 %	0.715
7	RSM5	0	2 %	0	2 %	1.188
8	RSM6	1	3 %	0	2 %	0.939
1	RSM7	-1	1 %	1	3 %	0.849
6	RSM8	0	2 %	1	3 %	1.456
3	RSM9	1	3 %	1	3 %	1.150

Table 4 Correlation matrix between the responses selected for the PB experiment.

Response	$Y_{PBD}$	$Y_{SBET}$	$Y_{Dp}$
$Y_{PBD}$	1	0.689**	-0.45
$Y_{SBET}$	0.689**	1	-0.828**
$Y_{Dp}$	-0.455	-0.828**	1

\*\* indicates correlations that are statistically significant.  $Y_{BD}$ : BD productivity;  $Y_{SBET}$ : BET specific surface area;  $Y_{Dp}$ : Average pore diameter.

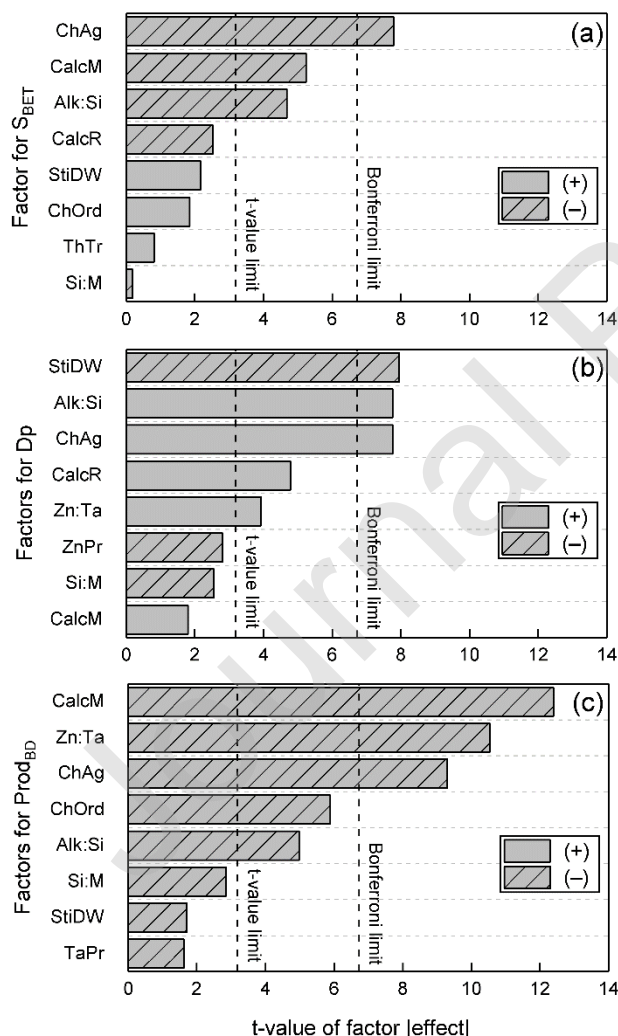


Fig. 3 Pareto chart of standardized effects each TUD-1 synthesis has on the selected responses: (a) butadiene productivity; (b) BET specific surface area; (c) Average pore diameter. In comparing

both levels, dashed bars indicate that the low level of the parameter gave the highest response; dash-less bars indicate the high level resulted in the highest response.

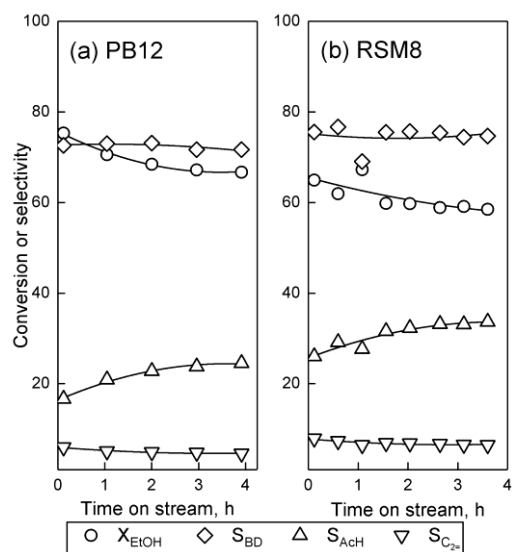


Fig. 4 Conversion and selectivity towards major products of ethanol conversion on (a) PB12 and over time.  $T = 350\text{ C}$ ,  $P = 1\text{ atm}$ ,  $WHSV_{EtOH} = 5.3\text{ h}^{-1}$ . EtOH: ethanol. AcH: acetaldehyde.  $C_{2=}$ : ethylene.

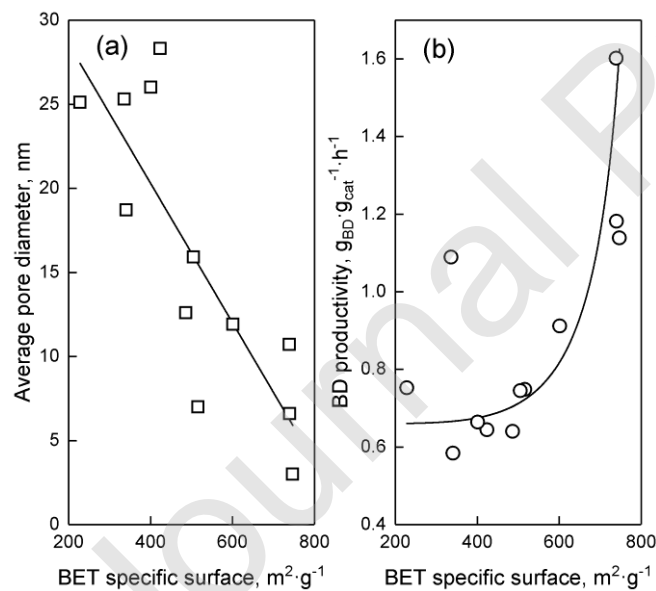


Fig. 5 Relationship between BET specific surface area and (a) the average pore diameter, (b) BD productivity of PB series of catalysts.

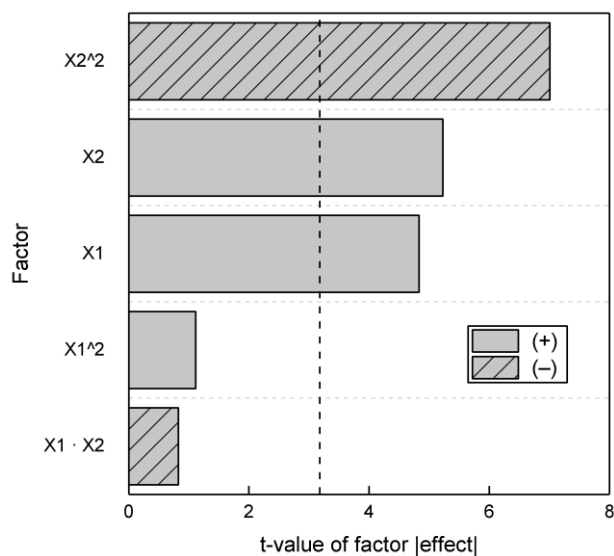


Fig. 6 Pareto chart of the standardized main and interaction effects the Zn and Ta content have on the BD productivity of Zn-Ta-TUD-1. X1 = Zn mol.%; X2 = Ta mol.%. In comparing both levels, dashed bars indicate that the low level of the parameter gave the highest response; dash-less bars indicate the high level resulted in the highest response.

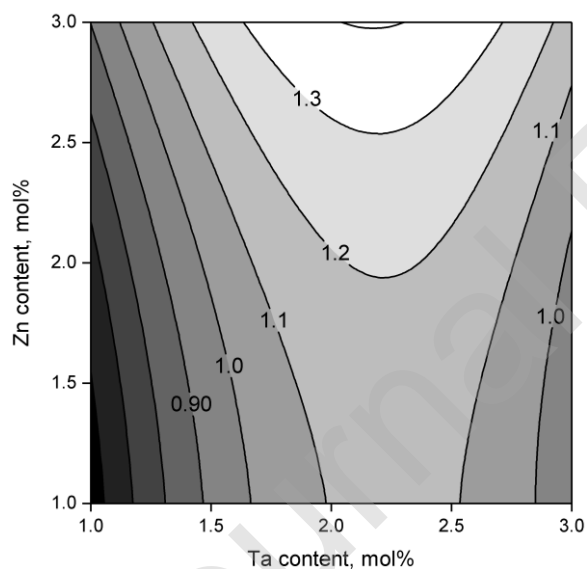


Fig. 7 Contour plot obtained by the RSM representing BD productivity versus Zn and Ta loading in TUD-1. BD productivity increases from dark to light on the gray scale. Reaction conditions: 350 °C,  $WHSV_{EtOH}$  of 5.3 h<sup>-1</sup>, TOS of 1 h.

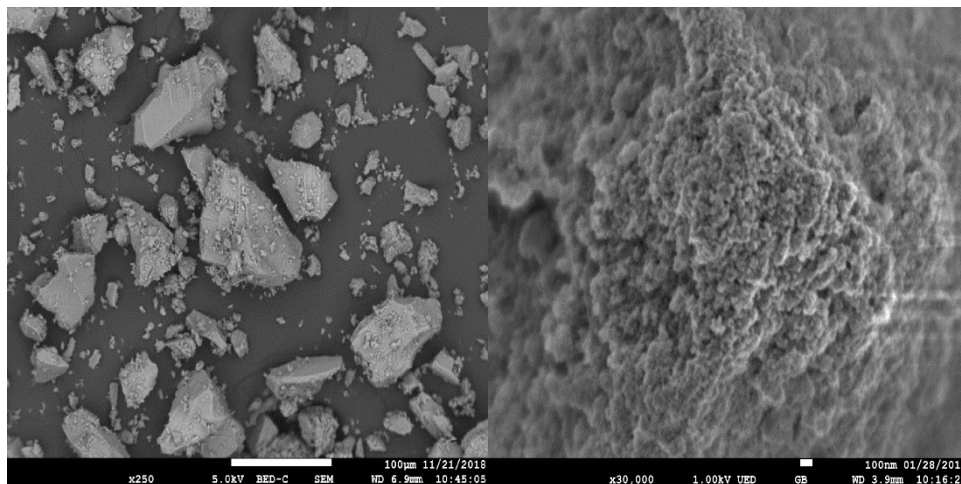


Fig. 8 SEM images at different magnifications of Zn-Ta-TUD-1 prepared during the RSM experiment.

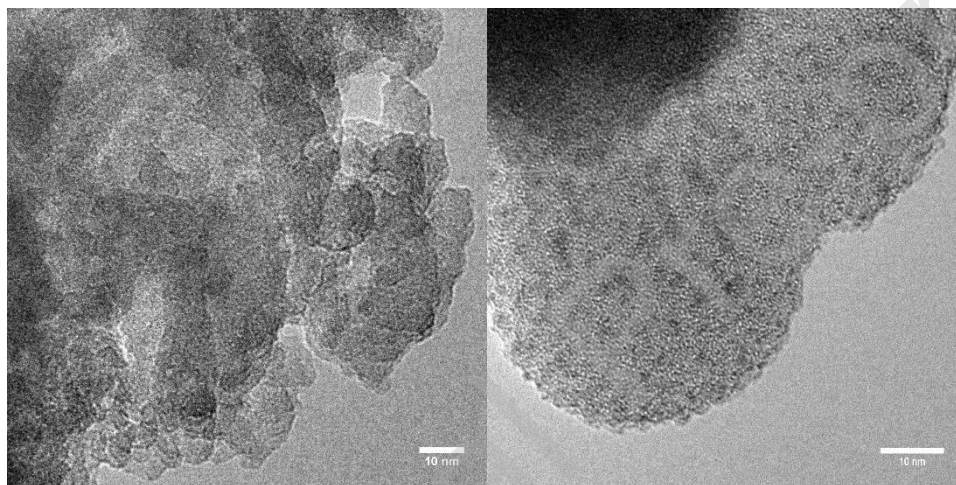


Fig. 9 HR-TEM images of Zn-Ta-TUD-1 prepared during the RMS experiment. Left: RSM9 image taken immediately. Right: the same area of RSM9 after irradiation under electron beam for 5 minutes.